

## SUPPLEMENTARY MATERIAL

### Role of zinc and magnesium ions in the modulation of phosphoryl transfer in protein tyrosine phosphatase 1B

Elisa Bellomo,<sup>a</sup> Asma Abro,<sup>b</sup> Christer Hogstrand,<sup>a</sup> Wolfgang Maret<sup>a,\*</sup> and Carmen Domene<sup>b,c,d,\*</sup>

<sup>a</sup> Departments of Biochemistry and Nutritional Sciences, King's College London, 150 Stamford Street, London, SE1 9NH, United Kingdom, <sup>b</sup> Department of Chemistry, King's College London, Britannia House, 7 Trinity Street, London SE1 1DB, United Kingdom, <sup>c</sup> Chemistry Research Laboratory, Mansfield Road, University of Oxford, Oxford OX1 3TA, United Kingdom, <sup>d</sup> Department of Chemistry, University of Bath, 1 South Building, Claverton Down, Bath BA2 7AY, United Kingdom

\*Corresponding authors: C.Domene@bath.ac.uk & wolfgang.maret@kcl.ac.uk

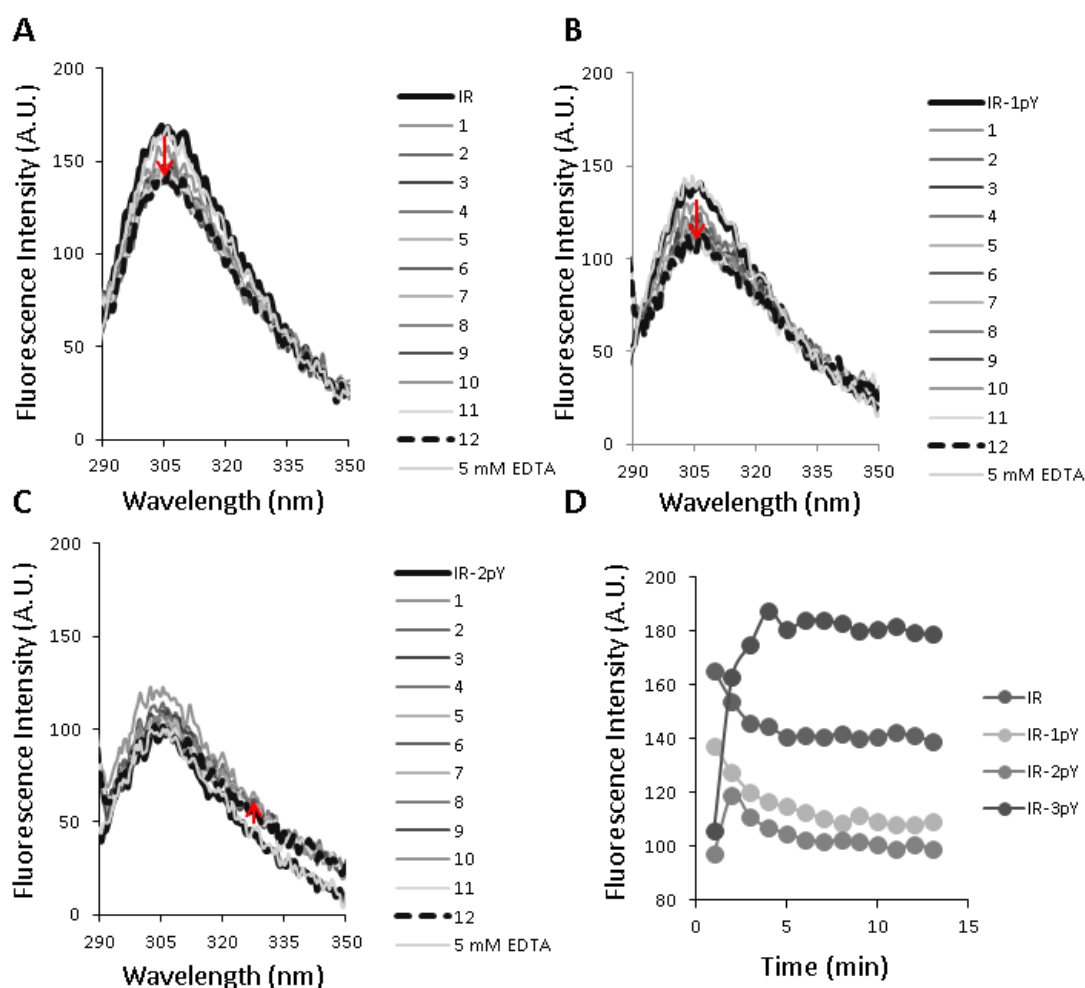


**Figure S1.** Zinc effects on the intrinsic fluorescence of phosphorylated insulin receptor (IR) peptides. 1 mM ZnSO<sub>4</sub> was added to 10 μM of dephosphorylated IR peptide (A), or IR peptide containing one (B), or two (C) phosphotyrosines. The sample was excited at 280 nm and emission spectra were collected every minute after zinc addition. At the end of each experiment, 5 mM EDTA was added. The maximum emission between 302 and 307 nm was averaged, and plotted against time (D).

**Table S1.** Simulation systems employed in this study using four PDB crystallographic structures of PTP1B and a control (1CAM).

SET	Protein Conformation	PDB ID	System	ASP181 Protonation State	Simulation time (ns)
1	Open (Apo)	2CM2	150 mM Zn <sup>2+</sup> solution	Charged	270
2	Open (Apo)	2CM2	150 mM Mg <sup>2+</sup> solution	Charged	155
3	Open (Apo)	2CM2	Docked Zn <sup>2+</sup> + in solution	Charged	175
4	Closed	3I80	150 mM Zn <sup>2+</sup> solution	Charged	170
5	Closed	3I80	150 mM Mg <sup>2+</sup> solution	Charged	155
6	Closed	3I80	150 mM Mg <sup>2+</sup> solution	Neutral	155
7	Closed	3I80	Docked Zn <sup>2+</sup> + in solution	Charged	155
8	Phospho-intermediate	1A5Y	150 mM Zn <sup>2+</sup> solution	Charged	155
9	Phospho-intermediate	1A5Y	150 mM Mg <sup>2+</sup> solution	Charged	155
10	Phospho-intermediate	1A5Y	Docked Zn <sup>2+</sup> + in solution	Charged	215
11	Control	1CAM	Zn <sup>2+</sup> in system	-	155
12	TS analog of PTP1B	3I7Z	150 mM Zn <sup>2+</sup> solution	Charged	110
13	Closed	3I80	150 mM Zn <sup>2+</sup> solution	Neutral	160
14	Closed with substrate	3I80	150 mM Zn <sup>2+</sup> solution	Neutral	155
15	Open (Apo)	2CM2	150 mM Zn <sup>2+</sup> solution + Zn <sup>2+</sup> manually placed in grid	Neutral	150
16	Open (Apo)	2CM2	150 mM Zn <sup>2+</sup> solution + Zn <sup>2+</sup> manually placed in grid	Charged	150
17	Closed	3I80	150 mM Zn <sup>2+</sup> solution + Zn <sup>2+</sup> manually placed in grid	Neutral	150
18	Closed	3I80	150 mM Zn <sup>2+</sup> solution + Zn <sup>2+</sup> manually placed in grid	Charged	150
19	Phospho-intermediate	1A5Y	150 mM Zn <sup>2+</sup> solution + Zn <sup>2+</sup> manually placed in grid	Neutral	150
20	Phospho-intermediate	1A5Y	150 mM Zn <sup>2+</sup> solution + Zn <sup>2+</sup> manually placed in grid	Charged	155
21	Closed with substrate	3I80	150 mM Zn <sup>2+</sup> solution + Zn <sup>2+</sup> manually placed in grid	Neutral	155
22	Closed with substrate	3I80	150 mM Zn <sup>2+</sup> solution + Zn <sup>2+</sup> manually placed in grid	Charged	150
23	Phospho-intermediate GLN262	1A5Y	150 mM Zn <sup>2+</sup> solution + Zn <sup>2+</sup> manually placed in grid	Charged	200
24	Phospho-intermediate GLN262	1A5Y	150 mM Mg <sup>2+</sup> solution + Mg <sup>2+</sup> manually placed in grid	Charged	200
Total simulation time (ns)					3950

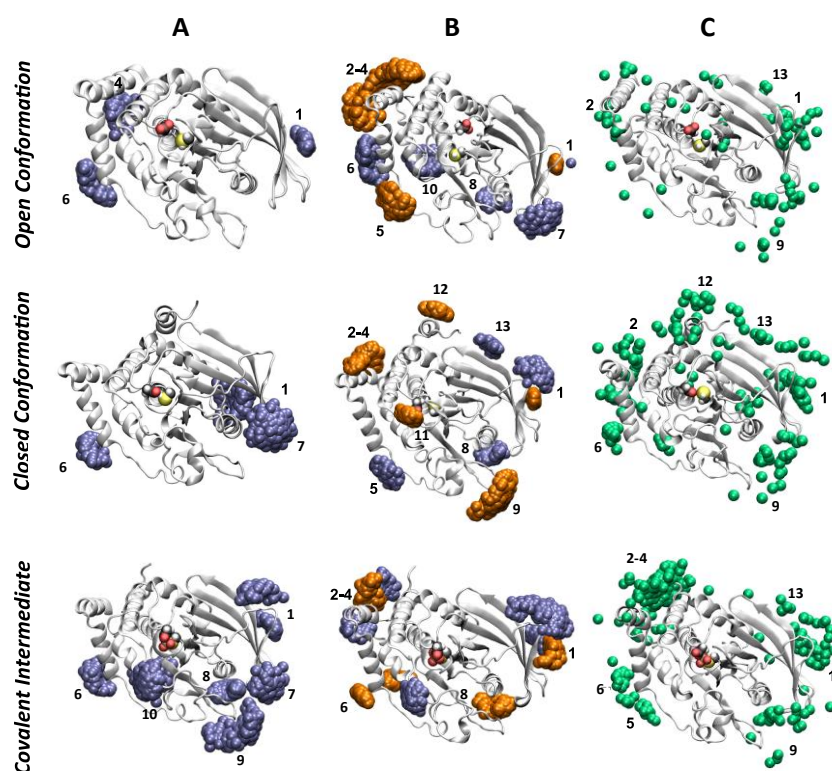


**Figure S2.** Snapshots of MD systems using the PTP1B open (PDB code: 2CM2), closed (PDB code: 3I80) and covalent intermediate (PDB code: 1A5Y) conformations, in the presence of  $\text{Zn}^{2+}$  (purple/orange) or  $\text{Mg}^{2+}$  (green). (A) Representative snapshots from the MD simulations where initial positions of ions are assigned at random.  $\text{Zn}^{2+}$  at a distance of 3 Å or less from the protein are shown in purple. (B) Initially docked  $\text{Zn}^{2+}$  are in orange and remaining  $\text{Zn}^{2+}$  at a distance of 3 Å or less of the protein are in purple. (C)  $\text{Mg}^{2+}$  at a distance of 3.5 Å or less from the protein are shown in green. Numbers displayed correspond to zinc ion binding sites based on the nomenclature employed by Bellomo et al.<sup>1</sup> Residues at the active site, Asp181 and Cys215, are shown as a van der Waals spheres with O atoms in red and S atoms in yellow.

### Parameterization protocol

Parameters for the cysteinyl phosphate (CSP) residue in the covalent intermediate (Figure S1) form were developed in-house. Parameters for the ligand to use in combination with the force-field potential of the rest of the system were generated in accordance with the CHARMM parameterization philosophy. Within the CHARMM force field, a novel CHARMM General Force Field (CGenFF) version 2b7<sup>2-4</sup> with a unified parameterization philosophy is available and was employed here. The cysteinyl phosphate parameters were based on cysteine, with novel parameters developed for the S-P junction, which was not found in the original CHARMM force field. The CHARMM partial charges of residue CSP were obtained from an initial consultation in the Paramchem library via version 0.9.7 of the CGenFF program at <https://cgenff.paramchem.org/>. They are based on cysteine and phosphate, with a total charge constraint of -2. Final partial charges are given in Table S2. The bonded and angular parameters of the S-P junction were optimized against QM target data extracted from the Hessian computed at the MP2/6-31+G(d) level of theory. The bonded parameter is given in Table S3, and the angles in Table S4. The two torsions C-S-P-O and C-C-S-P were scanned using QM calculations, at the MP2/6-31+G(d) level. The fitting is done with a special variant of the MCSA algorithm developed by Guvench and Mackerell<sup>5-6</sup> to simultaneously fit both dihedral parameters and minimise the RMS energy. These torsions are given in Table S5.

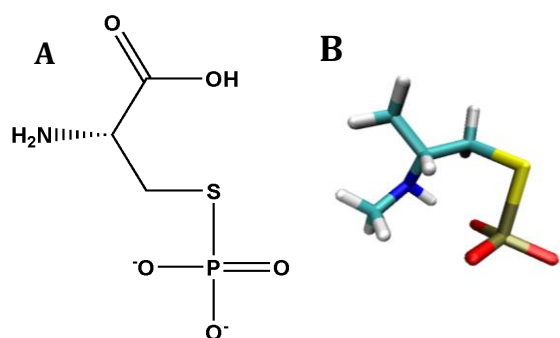


**Figure S3.** (A) CSP chemical structure, and (B) its licorice representation.

**Table S2.** CGenFF CSP partial charges

Name	Type	Charge
N	NH1	-0.47
HN	H	0.31
CA	CT1	0.07
HA	HB	0.09
CB	CT2	-0.48
HB1	HA	0.09
HB2	HA	0.09
SG	S	-0.36
P2	P2	1.30
O22	ON3	-0.88
O23	ON3	-0.88
O24	ON3	-0.88
C	C	0.51
O	O	-0.51

**Table S3.** CGenFF bond parameters for CSP

Bond	$K_b$	$b_0$ (Å)
S – P	87.07	2.23

**Table S4.** CGenFF angle parameters for CSP

Angle	$K_\theta$	$\theta$
C – S – P	223.00	100.00
S – P – O	83.25	102.03

**Table S5.** CGenFF torsional parameters for CSP

Torsion	$K_{chi}$	N	$\delta$
C – S – P – O	0.48	3	0.00
C – C – S – P	1.42	3	0.00

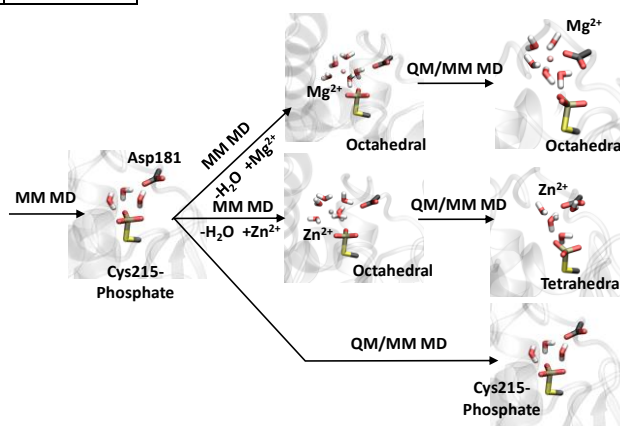


**Figure S4.** Schematic representation of the protocol followed to investigate the  $Zn^{2+}/Mg^{2+}$  coordination to PTP1B in the CSP intermediate. Residues Cys215phosphate, Asp181 and water molecules in the active site or coordinating the metal are shown in licorice representation.  $Mg^{2+}$  and  $Zn^{2+}$  are represented by a pink and grey sphere respectively. Protein secondary structural elements are shown as white transparent surfaces.

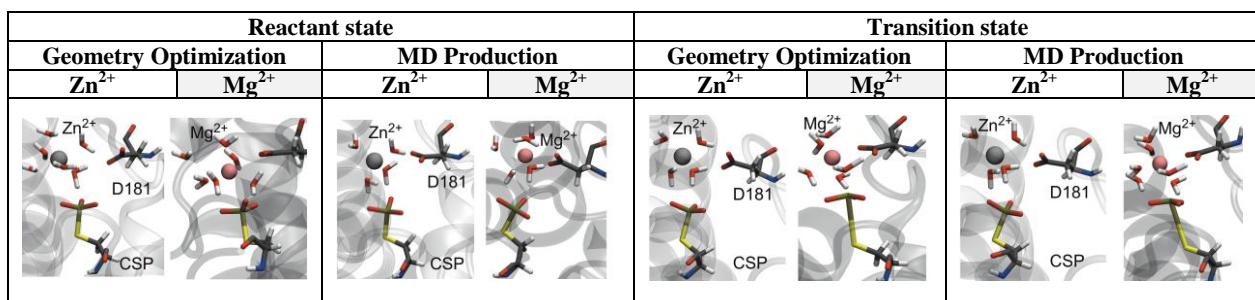


**Figure S5.** Active site of PTP1B (phosphorylated form) shown upon geometry optimization of reactants and transition state for Mg<sup>2+</sup> and Zn<sup>2+</sup> systems. The geometry optimized structure is compared to a representative snapshot from the production run for (B) reactants and (D) transition state. The transition state optimization was started from a snapshot of the QM/MM metadynamics simulation. Mg<sup>2+</sup> and Zn<sup>2+</sup> are represented by a pink and grey sphere respectively. Residues Cys215phosphate (CSP), Asp181 (D181) and water molecules in the active site or coordinating the metal are shown in licorice representation.

**Table S6.** Free-energy values obtained from metadynamics runs for the PTP1B enzymatic reaction. Energy values for reactant (R), product (P), secondary product (P') and transition state (TS) for the wild type (WT) system in the absence of ions and in the presence of Mg<sup>2+</sup> or Zn<sup>2+</sup> are reported.

System	Energy state (kcal/mol)		$\Delta G_{RP}$ (kcal/mol)	$\Delta G_{RP'}$ (kcal/mol)	$\Delta G^\ddagger$ (kcal/mol)	$\Delta\Delta G \text{ Mg}^{2+}\text{-WT}$ (kcal/mol)	$\Delta\Delta G^\ddagger \text{ Mg}^{2+}\text{-WT}$ (kcal/mol)
WT	R	-37	-3	+2	+18	+3	+5
	P	-34					
	P'	-35					
	TS	-19					
Mg <sup>2+</sup>	R	-61	-6	-24	+23		
	P	-55					
	P'	-36					
	TS	-38					
Zn <sup>2+</sup>	R	-42	-	-	+38		
	P	-					
	P'	-					
	TS	-4					

#### Comparison between active site catalytic residues and water molecules in the crystal structures, and representative snapshots from MD simulations (Figure S6).

In the closed conformation, two crystallographic water molecules were detected (W1 and W2). They form H-bonds with the Asp181 side chain and the NH backbone. Additional water molecules deep inside the active site are absent as vanadate is present as a TS analog of phosphate bound to Cys215 and Asp181, blocking access to the catalytic site. In addition to other water molecules that fill the active site pocket, water molecules in an orientation similar to those of W1 and W2 are observed in an MD simulation that lacks the TS analog vanadate. The crystal structure of the covalent intermediate shows three active site water molecules interacting with the phosphate group and Asp181. W2 is thought to be essential for dephosphorylation of the covalent intermediate.

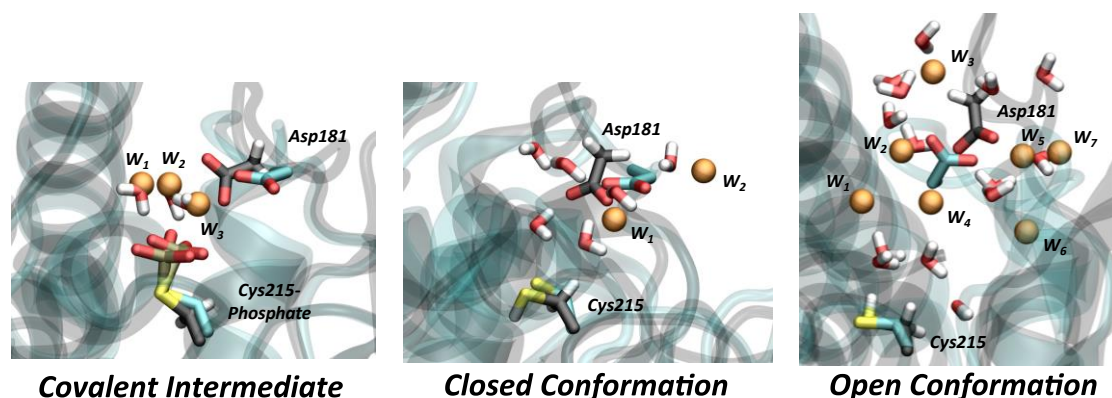


**Figure S6.** Comparison between active site catalytic residues and water molecules in the crystal structures, and representative snapshots from MD simulations. C atoms from X-ray or MD structures are shown in cyan and grey, respectively. O, H, and S atoms are shown in red, white and yellow, respectively. Crystallographic water molecules are shown in orange and labeled W<sub>n</sub> (n = 1 to 7).

## References

1. Bellomo, E.; Massarotti, A.; Hogstrand, C.; Maret, W., Zinc ions modulate protein tyrosine phosphatase 1B activity. *Metallomics* **2014**, *6* (7), 1229-1239.
2. Vanommeslaeghe, K.; Raman, E. P.; MacKerell, A. D., Automation of the CHARMM General Force Field (CGenFF) II: Assignment of Bonded Parameters and Partial Atomic Charges. *J Chem Inf Model* **2012**, *52* (12), 3155-3168.
3. Vanommeslaeghe, K.; MacKerell, A. D., Automation of the CHARMM General Force Field (CGenFF) I: Bond Perception and Atom Typing. *J Chem Inf Model* **2012**, *52* (12), 3144-3154.
4. Vanommeslaeghe, K.; Hatcher, E.; Acharya, C.; Kundu, S.; Zhong, S.; Shim, J.; Darian, E.; Guvench, O.; Lopes, P.; Vorobyov, I.; MacKerell, A. D., CHARMM General Force Field: A Force Field for Drug-Like Molecules Compatible with the CHARMM All-Atom Additive Biological Force Fields. *J Comput Chem* **2010**, *31* (4), 671-690.
5. Guvench, O.; Mackerell Jr, A. D., Computational evaluation of protein–small molecule binding. *Curr Opin Struct Biol* **2009**, *19* (1), 56-61.
6. Guvench, O.; Mackerell Jr, A. D., Automated conformational energy fitting for force-field development. *J Mol Model* **2008**, *14* (8), 667-679.